



## **Distributed fiber optic systems – application to strain measurement of post-tensioned concrete structures**

Mathieu Galan, Edouard Buchoud, Jean-Marie Henault, Frédéric Taillade, Karim Benzarti

### **► To cite this version:**

Mathieu Galan, Edouard Buchoud, Jean-Marie Henault, Frédéric Taillade, Karim Benzarti. Distributed fiber optic systems – application to strain measurement of post-tensioned concrete structures. European Journal of Environmental and Civil Engineering, 2024, pp.1-18. <10.1080/19648189.2024.2389155>. <hal-04750027>

**HAL Id: hal-04750027**

**<https://enpc.hal.science/hal-04750027v1>**

Submitted on 23 Oct 2024

**HAL** is a multi-disciplinary open access archive for the deposit and dissemination of scientific research documents, whether they are published or not. The documents may come from teaching and research institutions in France or abroad, or from public or private research centers.

L'archive ouverte pluridisciplinaire **HAL**, est destinée au dépôt et à la diffusion de documents scientifiques de niveau recherche, publiés ou non, émanant des établissements d'enseignement et de recherche français ou étrangers, des laboratoires publics ou privés.



HAL Authorization

## Distributed Fiber Optic Systems – Application to strain measurement of post-tensioned concrete structures

Mathieu Galan<sup>1</sup>, Edouard Buchoud<sup>2</sup>, Jean Marie Henault<sup>3</sup>, Frederic Taillade<sup>3</sup>, Karim Benzarti<sup>4</sup>

<sup>1</sup> Civil Specialist in Monitoring of Nuclear Civil Buildings, EDF DTG, Lyon, FRANCE

<sup>2</sup> Engineer in Monitoring of Hydraulic Civil Buildings, EDF DTG, Grenoble, FRANCE

<sup>3</sup> Research Expert in Physical Measurements, EDF R&D, Chatou, FRANCE

<sup>4</sup> Research Director at Université Gustave Eiffel, Navier Lab, Champs sur Marne, FRANCE

\*Corresponding Author, E-mail: [mathieu.galan@edf.fr](mailto:mathieu.galan@edf.fr)

**KEYWORDS:** *Optical fiber, civil monitoring, post-tension, containment*

### List of acronyms

Distributed Fiber Optic Sensing (DFOS)

Optical Fiber (OF)

Optical Fiber Cable (OFC)

Vibrating Wire Strain Gauge (VWSG)

Structural Integrity Tests (SIT)

Fourier Transform Infrared Spectroscopy – Attenuated Total Reflectance (IRTF-ATR)

Glass Transition Temperature (T<sub>g</sub>)

Differential Scanning Calorimetry (DSC)

Dynamic Mechanical Analysis (DMA)

### **Abstract**

This paper aims to showcase recent advances on Optical Fiber distributed strain measurement systems applied to concrete monitoring. It focuses on their ability to accurately quantify concrete strain in post-tensioned containment buildings of nuclear power plants under various conditions, including instantaneous concrete strain due to pressure tests, delayed concrete strain due to creep/shrinkage, and instantaneous concrete strain due to tendon rupture.

To achieve this, the study considers several mockups including the VeRCoRs building, a 1/3 scale prestressed concrete containment mockup equipped with a large number of monitoring systems. This mockup facilitates the testing and qualification of distributed measurement systems within concrete structures during both operational phases (for prestressing monitoring) and pressure tests (for measuring instantaneous strain/displacement under pressure). Additionally, a post-tensioned beam was specifically designed and fabricated to examine tendon re-anchorage after cutting.

Another objective is to assess various Optical Fiber Cables (OFC) from different suppliers to ensure reliable measurements. The study also aims to test different installation methods, such as embedding the OFC into concrete or attaching them to the external surface using various adhesives.

## 1. Introduction

In nuclear power plants, the containment building is a safety-critical part serving as the final barrier against the release of nuclear elements in the atmosphere in case of an accident (Naus, 2007). This structure is constructed of post-tensioned reinforced concrete to prevent concrete cracking. During construction, ducts are installed with rebars in the formwork before concrete is poured. Then, after concrete curing, tendons are threaded through the ducts, tensioned and anchored. In the nuclear French fleet, the ducts are grouted to prevent strand corrosion. While effective, this technical solution has the drawbacks of making the cables unmonitorable, impossible to re-tension and irreplaceable. Due to these limitations, rigorous control and monitoring of such structures are necessary during construction, throughout their operational life, and even during decommissioning. Structural Integrity Tests are conducted every ten years, during which the building internal pressure is increased to assess its mechanical behavior and check the air tightness. Over time, the compressed concrete and tensioned tendons may indeed be affected by creep and relaxation phenomena, potentially compromising containment performance. In France, all containment building are equipped with sensors to monitor strain and displacement over time (Simon et al., 2011). For example, Vibrating Wire Strain Gauges (VWSGs) are embedded in the concrete to measure local strain, and Invar Wires equipped with LVDT and pendulums are surface mounted to measure global displacement variations. Temperature sensors, such as thermocouples or thermos-resistances, are also installed to correct strain measurements from temperature effects. In addition to this traditional instrumentation, Distributed Fibre Optic Sensing (DFOS) is a powerful tool that enables strain and temperature measurement along an Optical Fiber Cable (Guemes et al., 2010). DFOS cables can be embedded in concrete during construction or surface mounted during the structure's service life and even in the decommissioning phase (Henault et al., 2011, 2012).

The metrological chain consists of an interrogator connected to an optical fiber. The fibre optic sensors operate based on electromagnetic wave backscattering. This involves launching a light pulse into the fibre optic. As the light interacts with the fibre optic, a small part is reflected back to the interrogator, resulting in a frequency shift and an amplitude that depend on the strain and temperature conditions.

Interrogators utilise three main effects: Rayleigh and Brillouin measurements are sensitive to temperature and strain, while Raman measurements are only sensitive to temperature. These devices provide temperature or strain profiles along the fibre, with parameters such as distance range, spatial resolution and an uncertainty depending on the interrogator technology. Typically, Raman interrogators provide temperature profile with uncertainties of a few tenth of °C over several kilometers. Brillouin devices offer a distance range of several kilometres, a spatial resolution of 50cm and a strain uncertainty of around  $\pm 20 \mu\text{m/m}$ , whereas Rayleigh devices have a distance range of 70m, a spatial resolution of 1cm and a strain uncertainty of around  $\pm 1 \mu\text{m/m}$ .

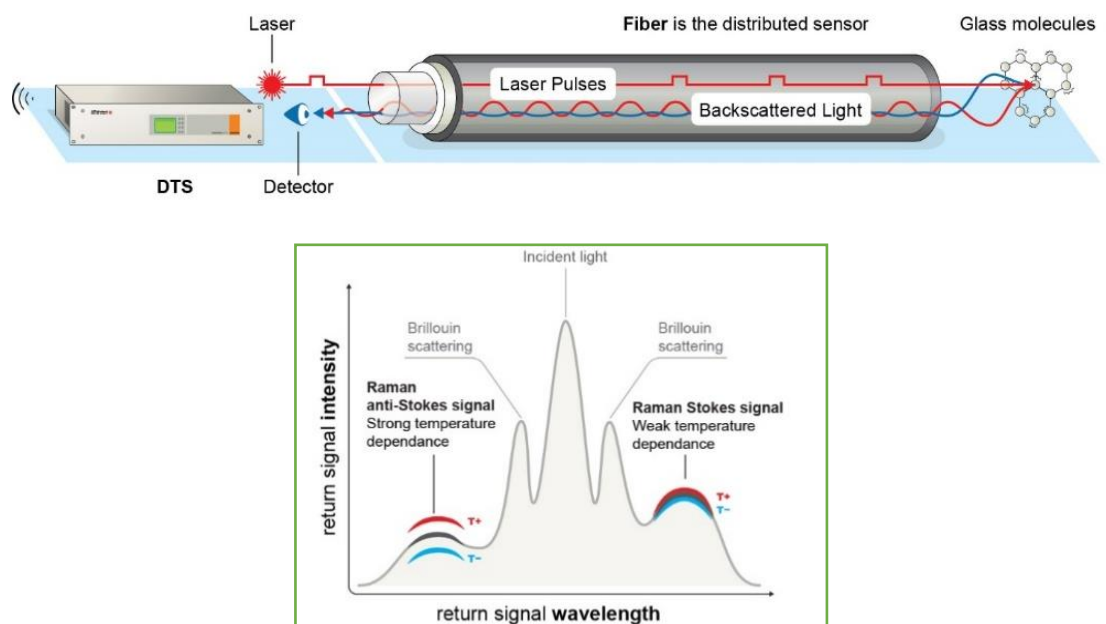


Figure 1. Distributed Optical Fiber Sensor principle showing the backscattered spectra: Rayleigh, Brillouin and Raman effects.

For both Brillouin and Rayleigh interrogators, the raw measurement is a spectral shift,  $\Delta\nu$ , linked to strain,  $\varepsilon$ , and temperature variation,  $\Delta T$ , between two fibre states, described by:

$$\Delta\nu(x) = C_\varepsilon\varepsilon(x) + C_T\Delta T(x)$$

Where  $C_\varepsilon$  and  $C_T$  are calibration coefficients ( $C_\varepsilon$  in MHz/ $\mu\varepsilon$  and  $C_T$  in MHz/ $^\circ\text{C}$ ).

This paper presents several findings on the application of DOFS for long-term monitoring of post-tensioned concrete structures. In the first part, we discuss results obtained for a 30m-high building equipped with DOFS, both embedded during construction 10 years ago and surface-mounted more recently. Different cables and adhesives were tested. Concrete instantaneous and delayed strain were evaluated with DOFS and compared with values obtained from traditional sensors. Given the necessity for sensors to remain efficient over decades, product durability is a crucial concern. Therefore, a dedicated study was initiated to assess the durability of various cables and adhesives. Furthermore, our research includes a specific study focusing on decommissioning aspects. A post-tensioned beam was built, and tendons were subsequently cut. DOFS allowed for the experimental evaluation of the anchorage length of grout tendons within the structure. These results were compared with Eurocode values and will guide future studies addressing the decommissioning of containment buildings, which is a critical challenge for the decades ahead.

## **2. VeRCoRs containment Mockup - qualification of Optical Fiber systems for instantaneous and delayed concrete strain measurements**

VeRCoRs (French acronym for “Realistic Verification of Reactor Containment”) represents a 1/3 scale mock-up of a nuclear double wall containment building, designed without any metallic liner (Charpin et al., 2022). This facility serves the following purposes:

- investigating the long-term behaviour of prestressed concrete,
- assessing the effect of concrete ageing on leak tightness,
- validating scientific and engineering tools,
- qualifying monitoring techniques (Oukhemmanou et al., 2016)
- 

Constructed in 2014-2015, this mockup continues to be operational with its heating system remaining continuously active, and a pressure test being conducted every year.

### **2.1. Description of the Fiber Optic systems installed on VeRCoRs**

For comparison and qualification purposes, hundreds of local concrete strain sensors (~300 Vibrating Wire Strain Gauges, noted VWSG) and temperature sensors were embedded and are used as references. A distributed optical fiber cable (AFL DNS-4804) with a length of 2 kilometers was embedded within the VeRCoRs concrete thickness (1 internal along the passive reinforcement layer, 1 close to the middle along the circumferential prestressed tendon, 1 external along the passive reinforcement layer). Additionally, around 200m of cables were recently bonded to the external surface of the internal containment. Figure 2 illustrates the locations of the reference and DFOS strain sensors.



Figure 2. Local and distributed concrete strain measurement systems on VerCoRs Mockup – VWSG at the left (blue color on the drawing) and Optical Fiber cables on the right (orange color on the drawing)

The Optical Fibers are interrogated using a Brillouin interrogator, whose metrological performance is associated with an estimated uncertainty of  $20 \mu\text{m/m}$  (compared to  $1 \mu\text{m/m}$  with a Rayleigh interrogator). The choice of Brillouin interrogator is motivated to demonstrate the capacity of such device for future industrial application on real civil buildings (monitoring length of hundred meters to some kilometers compared to lower than 100m with Rayleigh system, geometrical step for strain monitoring of around 50 cm sufficient for strain monitoring of large civil structures, compared to 1 cm for Rayleigh system).

Periodic pressure tests are conducted every year at nominal pressure 4.2 bars relative, equivalent to the Ten-year periodic Structural Integrity Tests (SIT), at the scale of the mockup.

Since SIT n°3 (2019) and SIT n°5 (2021), two optical fiber cables (model AFL DNS-4804) have been respectively bonded in the vertical direction (0 grade, full height) and in the tangential direction at mid-height (half perimeter from 100 to 300 grades at +9 m). These two cables are glued to the external concrete wall of the Internal Containment, using epoxy adhesives (Sikadur 30 from Sika Company and Scotch-weld DP460 from 3M company).

Since SIT n°6 (2022), two other types of Optical Fiber Cables (OFC), namely Solifos v1 and Neubrex FN-SILL-4, have been bonded to the external concrete wall of the Internal Containment, using 2 different epoxy adhesives (Scotch-weld DP460 from 3M company and Sikadur 30, with thermal expansion coefficient respectively  $60$  to  $160 \mu\text{m/m}^\circ\text{C}$  and  $25 \mu\text{m/m}^\circ\text{C}$ ). The objective was to qualify these OFC in comparison to the AFL cable previously installed.

Figure 3 shows pictures of the various OFC considered in this experimentation, while Figure 4 illustrates the same OFC that have been bonded to the surface of the internal containment.



Figure 3. Pictures of the various Optical Fibers Cables tested on VeRCoRs mockup

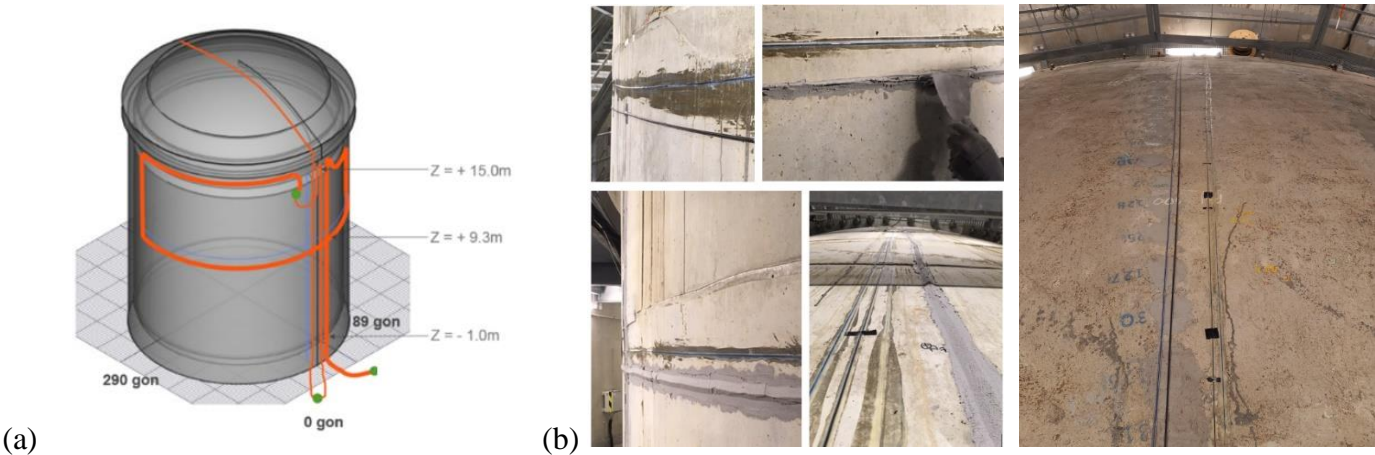


Figure 4. Distributed optical fiber strain sensors bonded to the external face of the internal containment on VeRCoRs Mockup (a), and pictures of the OFC glued with the 2 types of epoxy adhesives, scotch-weld DP 460 and Sikadur 30 (b).

Overall, the primary objective of this research is to validate the capability of the Optical Fiber systems to measure the short-term (pressure tests) and long-term (prestressing losses) behaviors of prestressed concrete containments with a high level of confidence. This involves assessing different installation configurations, including embedding the cables into the concrete, and gluing them onto the external faces considering various types of OFC and adhesives. All the monitoring systems are not installed at the same period (some were embedded into the concrete during construction, some were glued more recently), but for the comparison purpose of strain measurements between each device, this difference of installation period is not detrimental. During pressure tests, the reference instant is considered at the beginning of the test, when pressure is equal to 0. During operation, the delayed concrete strains trends can be compared using a common origin time, for example the time when the glued system was installed.

2.2. Measurement of the instantaneous strain during Structural Integrity Tests

Figure 5 presents the tangential strain profiles collected using the OFC embedded in the concrete at +9m and the OFC glued on the external concrete surface (at the same height), during the nominal pressure stage of SIT n°6. These profiles are compared to the measurements from the embedded VWSG located between heights of +7.5m and +9m.

Prestressing rib 1      Equipment Hatch      Prestressing rib 2



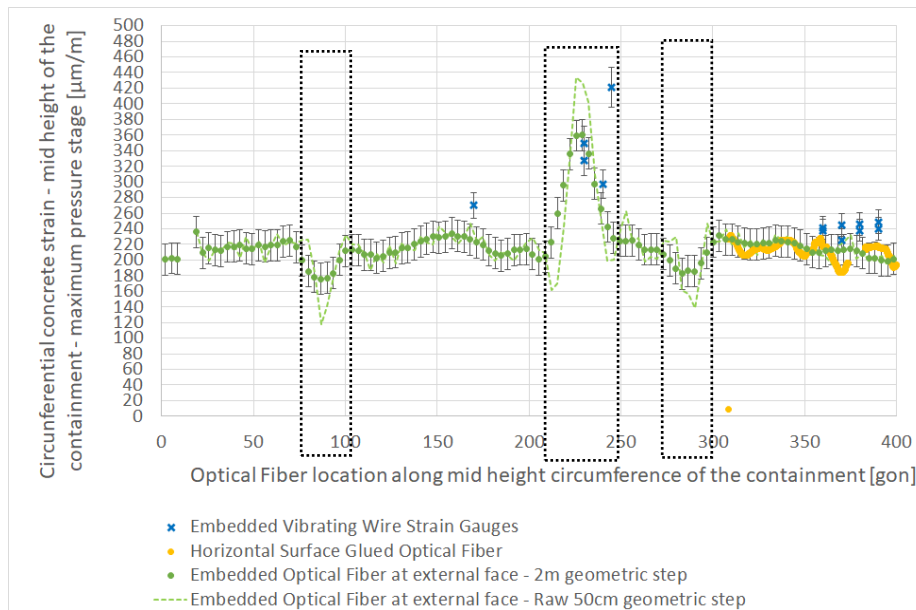


Figure 5. Circumferential concrete strain measured with VWSG, Glued and Embedded Optical Fiber Cables [ $\mu\text{m/m}$ ], at the mid height of the containment and during the maximum pressure stage of SIT N°6

The following observations are noted:

- Strains measured with both glued OFC and embedded OFC are consistent, showing differences on the order of  $\pm 10 \mu\text{m/m}$  (standard deviation). A more notable deviation is observed between OFC and VWSG measurements close to the equipment hatch at 250gr. In this singular area, the tangential strains values vary significantly with the distance to the hatch axis. Consequently a few uncertainty in the geometric location of the VWSG leads to a potential notable gap in the strains amplitudes. The most important point to note in this singular area is that the maximum value measured by OFC in tangential direction is in a good agreement with the ones measured by VWSG
- The distributed strain system demonstrates its capability to confidently measure strain profiles in specific areas, such as around the hatch (200-250 gr), providing complementary data to local measurements obtained with VWSG.
- A very good correlation of tangential strain in the cylinder is observed, between the embedded OFC interrogated with Brillouin, the glued OFC interrogated with Rayleigh and the embedded VWSG in the current area of the containment.

Figure 6 displays strain measurements as a function of pressure during SIT n°6. The strain level at the maximum pressure value, as well as the linearity and reversibility of the behavior are consistent between OFC and VWSG.

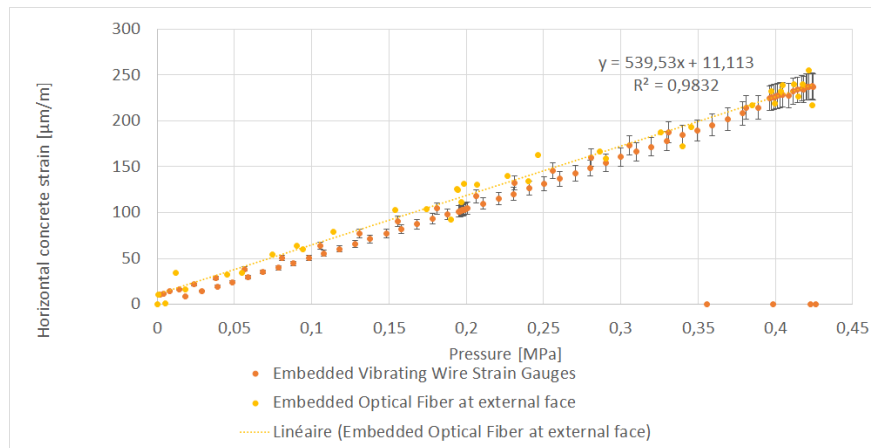


Figure 6. Concrete strain measured with VWSG and Embedded Optical Fiber [μm/m] versus pressure [MPa], at the mid height of the containment during SIT N°6

For comparison with the global measurements of radial displacements provided by the pendulums, strain profiles obtained from OFC are integrated over the entire horizontal measurement length ( $L$ ) of the Optical Fiber. Consequently, the variation of radial displacement  $\Delta R$  induced by the tangential strains of the Optical Fiber  $\varepsilon_i$  at each measuring step  $x_i$  (constant value equal to around 0.4m) is calculated using the formula  $R/L \cdot \int_0^L \varepsilon_i \cdot dx_i$ , where  $R$  is the radius of the containment.

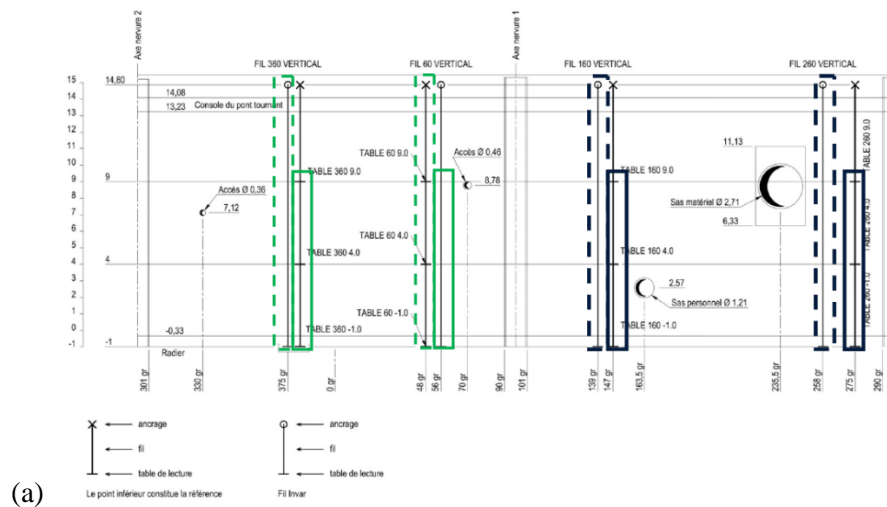


Figure 7. Locations of the considered pendulums/invar wires (a) and pictures of the utilized devices (b)

Figure 8 compares the displacement values between pendulums and OFC, demonstrating good consistency, with differences arising from the uncertainties inherent in both measuring systems.



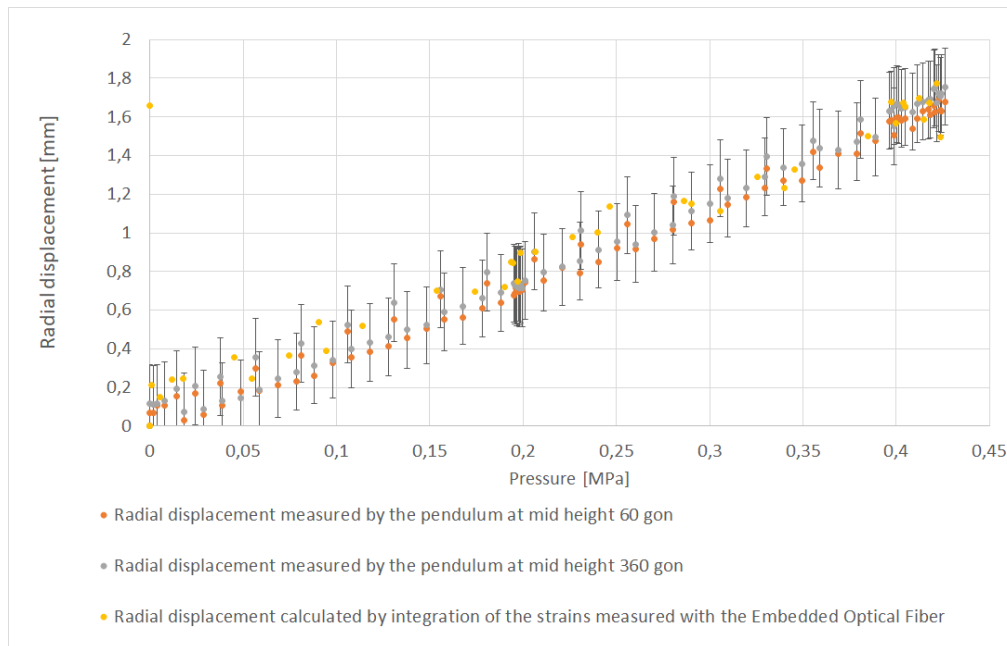


Figure 8. Concrete strain measured with the embedded Optical Fiber Cable integrated over the entire length [mm] versus pressure [MPa], in comparison to mid height pendulums during SIT N°6

NB on figure 8 : Zero value of radial displacements measured with pendulums is superimposed on the zero value of OFC).

The measurement uncertainty of radial displacement obtained by integration of optical fiber measurements is of the order of  $\pm 0.2\text{mm}$  (uncertainty of optical fiber concrete strain  $\pm 20\text{ }\mu\text{m/m}$  multiplied by the radius of the structure  $R=7.7\text{m}$ ).

### 2.3. Comparative analysis with different types of OFC and adhesives

Vertical OFC are glued on the whole vertical height of the containment, for qualification purpose of different cables and glue types.

Figure 9 compares the vertical strain profiles measured by various OFC bonded on the concrete surface using the 3M DP460 adhesive, with the strain values provided by the VWSG. The following observations can be made:

- A strong correlation in vertical strain values is found among the different types of OFC (AFL DNS 4804, Solifos v1 and Neubrex FN-SILL-4) bonded to the external concrete face and the embedded VWSG,
- The average differences between the different OFC types range from 10 to  $20\text{ }\mu\text{m/m}$ , indicating consistent measurements. However, both glued AFL and NEUBREX demonstrate strain values closer to VWSG measurements compared to bonded Brugg Solifos,
- The optical fiber distributed systems enable continuous strain profiles, unlike the local values provided by VWSG sensors. This is advantageous in areas with significant strain variations, such as near singular areas like the gusset at the bottom of the containment.

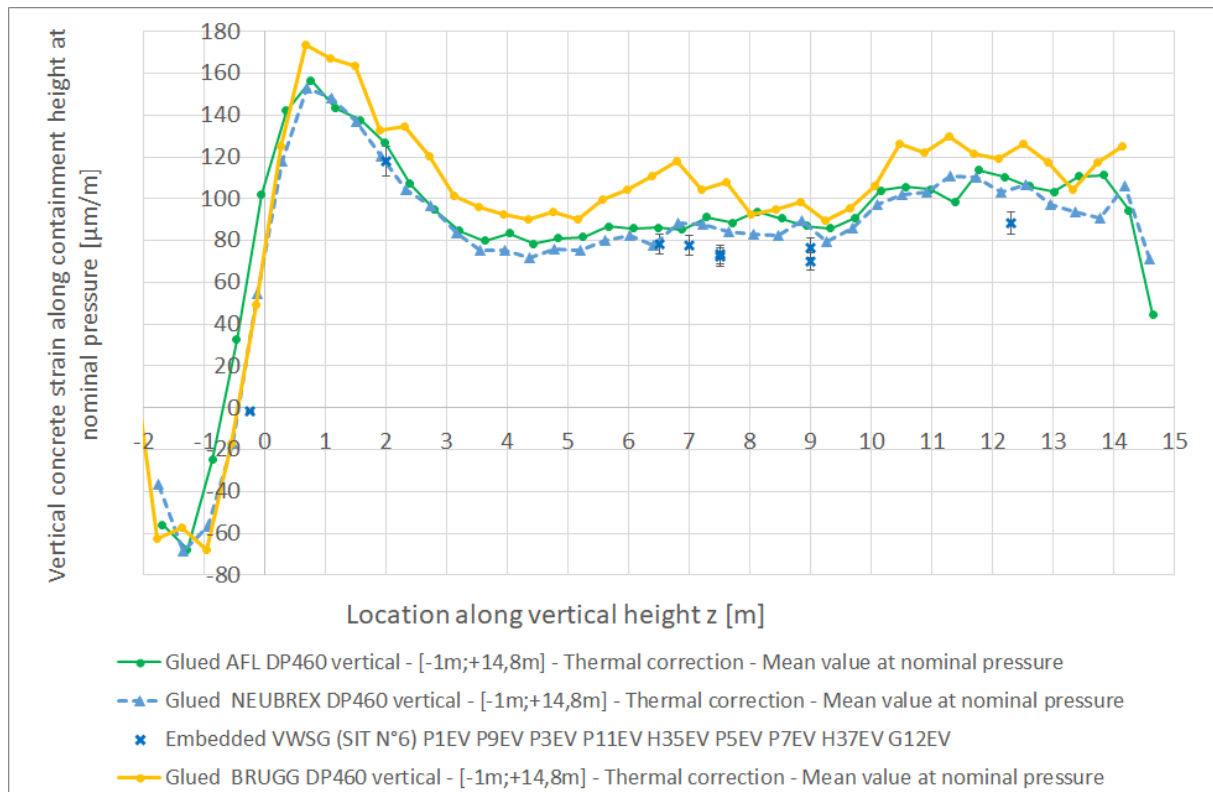


Figure 9. Vertical concrete strain measured with the various OFC (AFL/Solifos/Neubrex) bonded with the 3M DP460 adhesive and compared to VWSG values [μm/m], at the mid-height of the containment and during the maximum pressure stage of SIT N°6 (with uncertainty of the order of  $\pm 20$  μm/m).

Figure 10 compares the vertical strain profiles measured by each of the OFC bonded on the concrete surface for both Sikadur 30 and 3M DP460 adhesives, with the strain values provided by the VWSG. The following observations can be made:

- A strong correlation in vertical strain values is found among the different types of OFC (AFL DNS 4804, Solifos v1 and Neubrex FN-SILL-4) bonded to the external concrete face and the embedded VWSG,
- The average differences between the different OFC types range from 10 to 20 μm/m, indicating consistent measurements. However, both glued AFL and NEUBREX demonstrate strain values closer to VWSG measurements compared to bonded Brugg Solifos,
- The optical fiber distributed systems enable continuous strain profiles, unlike the local values provided by VWSG sensors. This is advantageous in areas with significant strain variations, such as near singular areas like the gusset at the bottom of the containment.

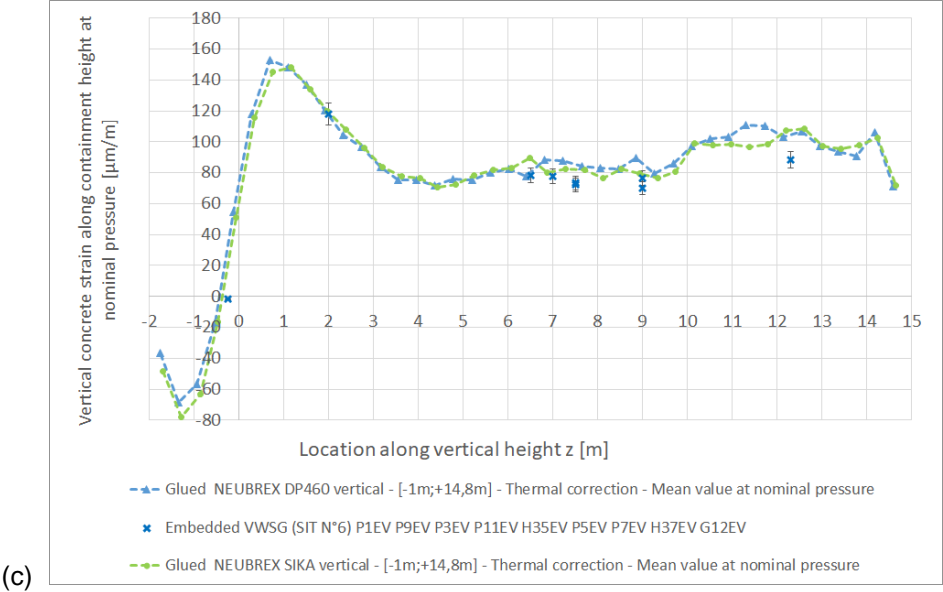
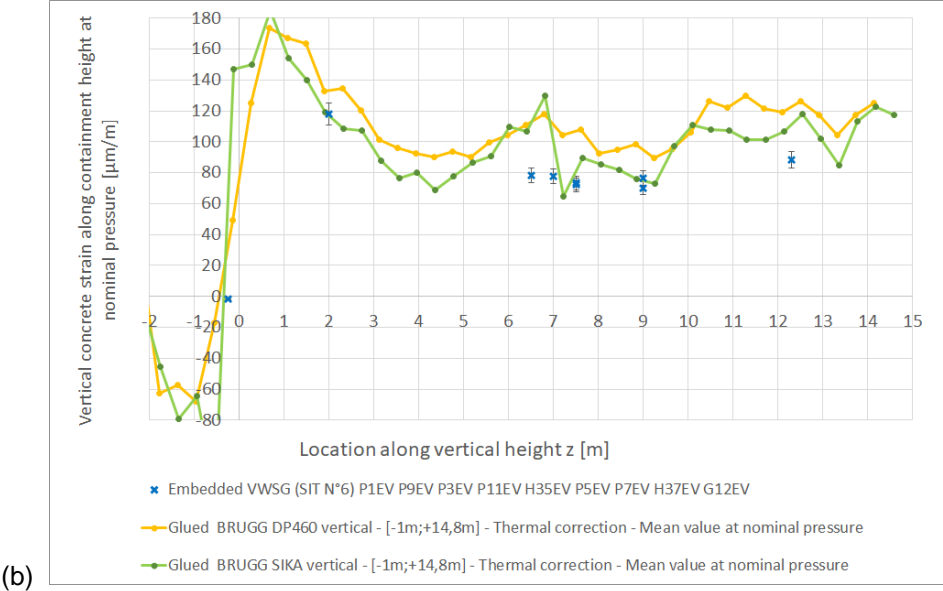
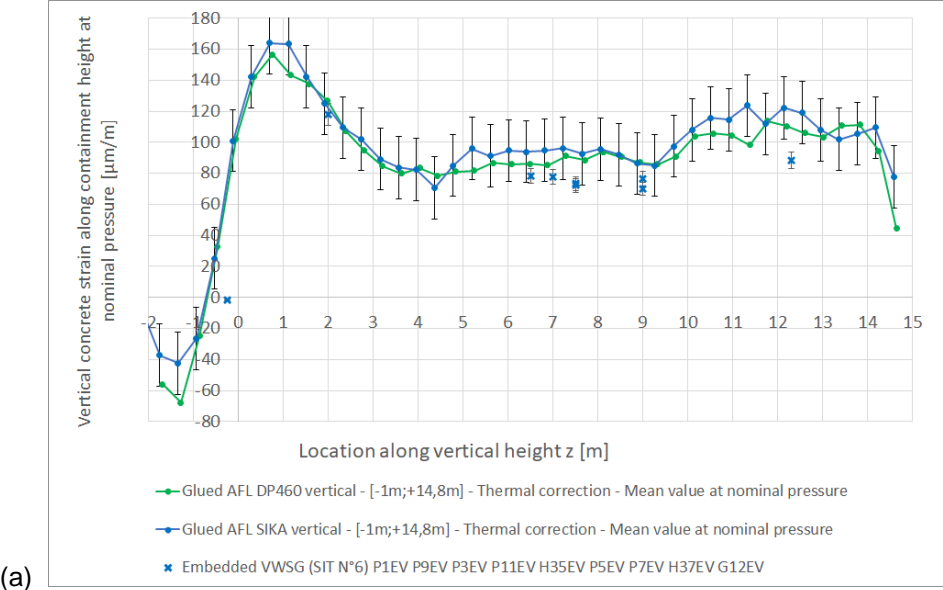


Figure 10. Vertical concrete strain measured with AFL (a), Brugg/Solifos (b) and Neubrex (c) OFC bonded with the two types of adhesives (Sikadur 30 and DP 460), and compared to VWSG values [ $\mu\text{m}/\text{m}$ ], at mid-height of the containment and during the maximum pressure stage of SIT N°6.

#### 2.4. Delayed concrete strains under shrinkage/creep since 2015 - Post processing of embedded tangential optical fiber

For long-term monitoring, the influence of temperature on strain measurements cannot be disregarded. Thus, thermal correction becomes imperative to correct the data from reversible thermal effects. The thermal correction method relies on a multilinear statistical model primarily incorporating time and temperature variables. This is the same kind of thermal correction model used for reversible effects on dams (Willm and Beaujoint, 1967).

In Figure 11, tangential strains measured by embedded OFC at the height of +4m, and corrected from thermal effects, are compared to the measurements of VWSG embedded in the current area of the containment mockup (respectively at heights ranging from +4m to +9m, near the external face).

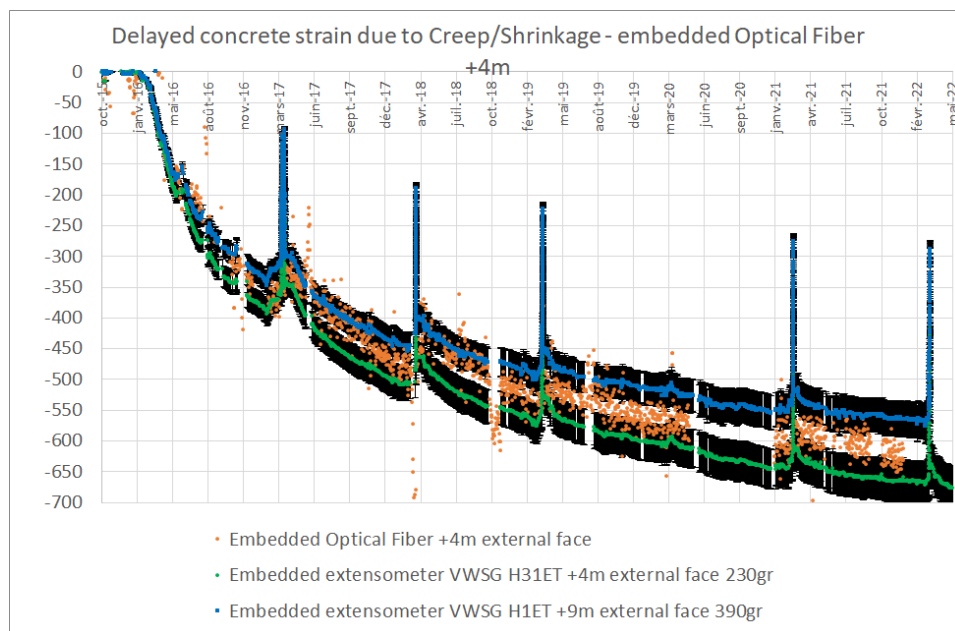


Figure 11: Strain measurements (corrected for thermal effects) versus time, as provided by OFC embedded in concrete at a height of 9m averaged over the circumference (excluding Equipment Hatch) (in orange), and by embedded VWSG (in blue/green).

From the graph, the following conclusions can be drawn:

- The creep measured by the embedded OFC between October 27th, 2015 (after the completion of prestressing and before the start of containment mockup heating) and early 2022, is around  $-600 \mu\text{m}/\text{m}$ . This value is comparable to the creep measured by the embedded VWSG, which ranges from  $-550 \mu\text{m}/\text{m}$  to  $-650 \mu\text{m}/\text{m}$  in current area of the containment, with a measurement uncertainty of approximately  $\pm 5\%$  of the total amplitude of the delayed concrete strains (Galan, 2022).
- Concrete strain rates measured by embedded OFC are comparable to those measured by embedded VWSG extensometers regardless of the analysis period. This includes both the period of strong creep after heating begins in March 2016 and the relatively damped creep period between SIT n°5 and SIT n°6, years 2021-2022).

### 3. Experimental program for durability qualification

For the qualification purpose of Optical Fiber technology in exterior conditions, an additional experimental program is needed to assess the behavior and properties of the cable and glue.

#### 3.1. Ongoing investigation on adhesive solutions for OFC bonding

EDF and Gustave Eiffel University (UGE) are collaboratively conducting a complementary program aimed at identifying an adhesive solution for securely bonding fiber optic cables to concrete surfaces.

The desired properties for the adhesives are as follows:

- Excellent adhesion to both concrete surfaces and the external sheath of fiber optic cables.
- Consistency suitable for vertical bonding, including characteristics such as thixotropy and creep control,
- Minimal variation in rigidity and stiffness throughout the entire operating temperature range is crucial, necessitating specific requirements for the glass transition temperature ( $T_g$ ). When the temperature exceeds  $T_g$ , the mobility of macromolecular chains increases significantly, causing a substantial drop in the adhesive's mechanical properties. Therefore, a minimal  $T_g$  value of  $\sim 75^\circ\text{C}$  is requested for maintaining consistent mechanical properties up to  $60^\circ\text{C}$ . Furthermore, the adhesive should exhibit a Young's modulus exceeding 1 GPa up to  $60^\circ\text{C}$ . Polymerization should occur under ambient conditions to eliminate the need for artificial heating on-site after installation,
- Expansion coefficient should closely match that of concrete ( $8\text{--}15\ \mu\text{m/m}^\circ\text{C}$ ).
- Durability under operational conditions is also essential for ensuring long-term performance of the bonded fiber optic instrumentation.

Based on these specifications, a preliminary selection of potential candidate adhesives has been chosen from the available products on the market. An important aspect of the study focuses on examining how curing conditions impact the Glass Transition Temperature ( $T_g$ ) and mechanical properties of these adhesives. Accordingly, the adhesives are subjected to various curing conditions such as ambient temperature curing in the laboratory, post-curing treatments at elevated temperatures, or exposure to real-world outdoor conditions. Systematic characterizations are then conducted using Differential Scanning Calorimetry (DSC) to determine their  $T_g$ , and Dynamic Mechanical Analysis (DMA) to assess the evolution of the tensile storage modulus (closely related to the material's Young's modulus) across the entire service temperature range.

These experiments are still ongoing, but the initial results reveal the following trends:

- For all adhesive systems, ambient curing at  $20^\circ\text{C}$  in the laboratory yields low  $T_g$  values, approximately around  $50^\circ\text{C}$ , suggesting an incomplete crosslinking process. The degree of cure remains generally below 90%.
- An appropriate post-heating cycle enables achieving the desired criterion for  $T_g$  ( $T_g$  close to  $75^\circ\text{C}$  or higher). For example, Figure 12 illustrates the influence of post-curing temperature (for a period of 1 hour) on the  $T_g$  values for two specific adhesives tested: Scotch-Weld DP 460 and DP 490, both commercially available from 3M. Increasing the post-curing temperature yields higher  $T_g$ , reaching a peak value, noted  $T_{g\text{max}}$ , where the polymer network is fully crosslinked (degree of cure close to 100%). Specifically, for DP 460 and DP 490,  $T_{g\text{max}}$  values of  $74^\circ\text{C}$  and  $81^\circ\text{C}$ , respectively, were achieved after 1 hour of post-curing at  $90^\circ\text{C}$  and  $70^\circ\text{C}$ . However, at higher post-curing temperatures, a decrease in  $T_g$  attributed to thermal degradation is observed for these two adhesives, with DP 490 showing a more pronounced effect. Nevertheless, this phenomenon is not consistently observed across all the adhesive systems studied, and such degradation does not occur within the service temperature range.
- Since implementing controlled post-curing on-site using a heating device is a quite complex task, it is anticipated that a natural post-curing process can occur when the adhesive is exposed to weather conditions, including seasonal temperature and moisture fluctuations, UV exposure, etc. To confirm this hypothesis, the experimental program involves exposing the selected adhesives to outdoor conditions for an extended duration, either fully exposed or shielded from

direct sunlight and rainfall under a thin concrete slab. For instance, in the case of adhesive DP 460, DSC characterizations demonstrated that a 6-month exposure in the field—including the summer season with external temperatures reaching 40°C—resulted in an increase in  $T_g$  from an initial value of 49°C to approximately 71°C (close to  $T_{g_{max}}$  of the system), irrespective of the type of exposure (full or sheltered). This finding indicates that the crosslinking process continues during outdoor exposure, facilitating an effective natural post-cure and enabling attainment of the  $T_g$  criterion (close to 75°C) within a few months. Furthermore, Figure 13 illustrates the DMA characterizations obtained for DP 460 adhesive samples exposed for 6 months in the field (full exposure or under shelter), compared to specimens cured in the laboratory at 20°C. The storage modulus versus temperature curves indicate that the exposed samples maintain a high level of stiffness up to 60°C, as required by industrial standards, unlike the samples cured at 20°C. In general, the six-month exposure period in the field demonstrates similar effects to those of the thermal post-cure for one hour at 90°C, in terms of crosslinking advancement for this particular adhesive.

In conclusion, this test program on polymer adhesives has demonstrated that the  $T_g$  value of the fully crosslinked adhesive ( $T_{g_{max}}$ ) is a crucial parameter for the reliability of bonded FO instrumentation. A value of  $T_{g_{max}}$  of at least 75°C is necessary to ensure that natural post-curing can be effective in the field, with the objective of maintaining consistent mechanical properties of the adhesive joint within the entire service temperature range.

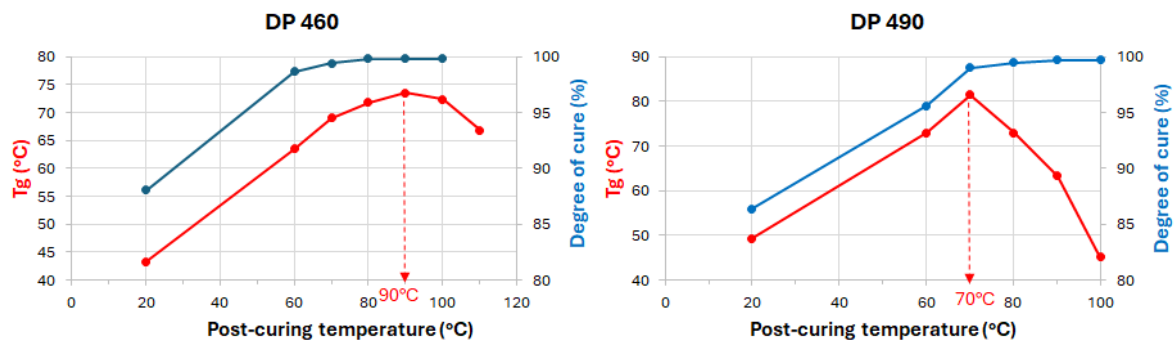


Figure 12: Influence of the post curing temperature (cycle duration of 1 hour) on the glass transition temperature ( $T_g$ ) and degree of cure of 2 peculiar adhesives, Scotch-weld DP 460 (a) and DP 490 (b)

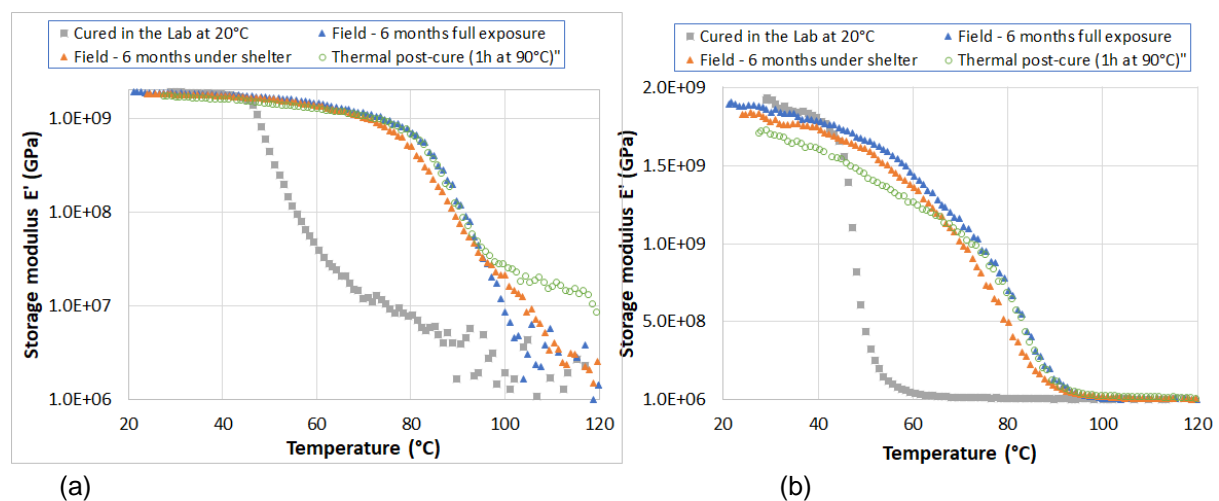


Figure 13. Variation of storage modulus ( $E'$ ) with temperature: DMA analysis of DP460 adhesive under different curing conditions. Logarithmic (a) and linear (b) scale representations.



### 3.2. Durability program on OFC

Previous research conducted by Alj et al. (2022) emphasized a straightforward "disqualifying" test, which involved immersing the Optical Fiber Cables in an alkaline solution (pH~13) at 60°C for several months. This test performed by EDF monitored various properties of the cable, including dimensions, tensile properties of the external coating, and interface properties among the different component materials of the sensors. Besides, a key aspect of this test was to ensure the watertightness of the cable end in the solution, preventing the infiltration of alkaline fluid into the cable and avoiding unexpected aging and degradation phenomena within it.

Figure 14 illustrates the implementation of this "disqualifying" test for the various Optical Fiber Cables used in the instrumentation of VeRCoRs mockup, focusing on the dimensional variations during immersion in the alkaline solution.

It is observed that the Neubrex cable undergoes slight swelling in both directions of the rectangular shape of its external sheath. This phenomenon is reversible, as the dimensions decrease after drying. This behavior is deemed acceptable, as it enhances confinement in the concrete, thereby improving adhesion. It should be noted that physicochemical analyses were conducted on the same Neubrex cable by Alj et al (2022) revealing slight degradation on the surface of the exterior coating (as indicated by analysis) during immersion at 40°C and 60°C in an alkaline solution. It's important to highlight that these IRTF-ATR results analyze the extreme surface of the sheath (with a penetration depth of the IR in the material of about 1  $\mu\text{m}$ ). Therefore, they reveal active chemical degradation at the surface of the sheath in contact with the alkaline solution, which may not necessarily be present or as pronounced in the thickness of the sample.

For AFL and Brugg cables, a slight and consistent decrease in the external coating diameter is observed, which could potentially result in reduced confinement within the concrete and a decrease in bonding.

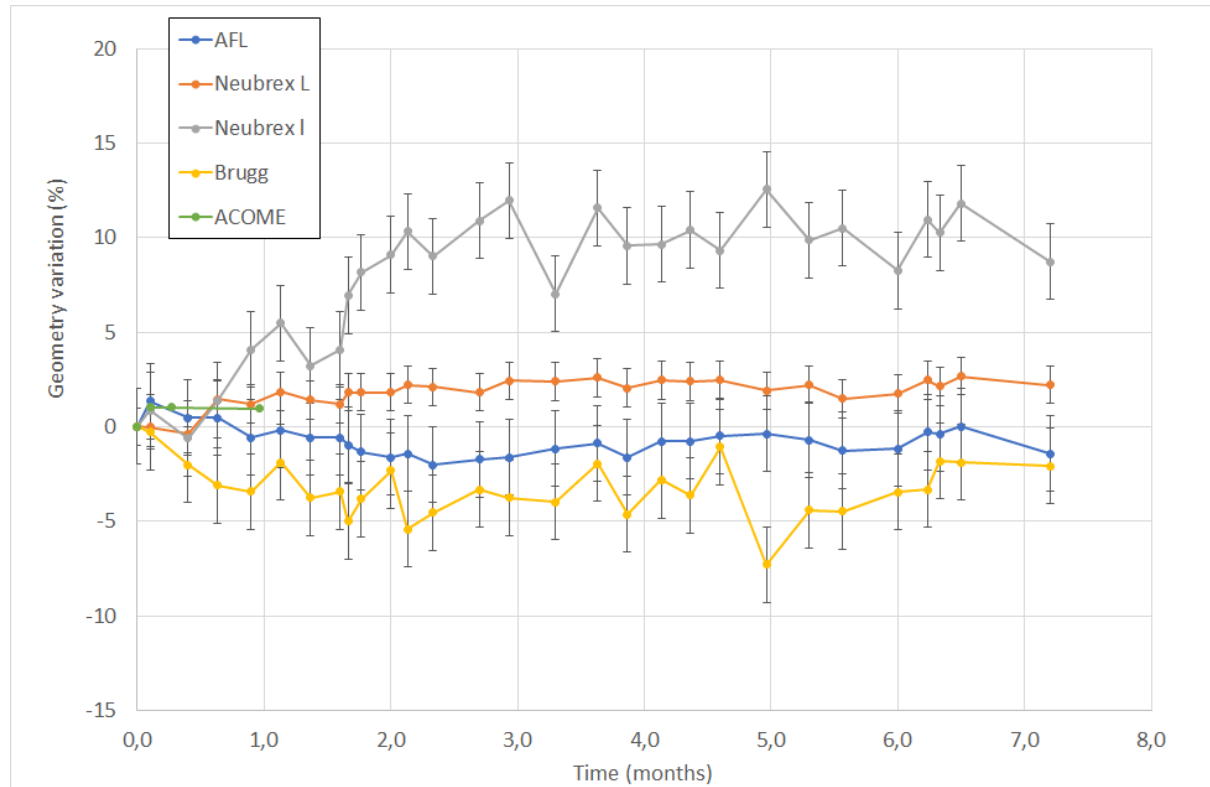


Figure 14. Dimensional changes of cables used for instrumentation in VeRCoRs mockup during exposure to alkaline solution at 60°C. 'L' and 'I' denote the larger and smaller lengths, respectively, of the rectangular section of the Neubrex cable.

However, this slight reduction is deemed acceptable due to the operational experience with AFL cables, notably in VeRCORs, where they were embedded in concrete for 10 years without any abnormal behavior. Additionally, the instantaneous and delayed concrete strains remained consistent with all other monitoring devices (such as VWSG, pendulums, invar wires), with no measurement drift observed for the embedded AFL cables.

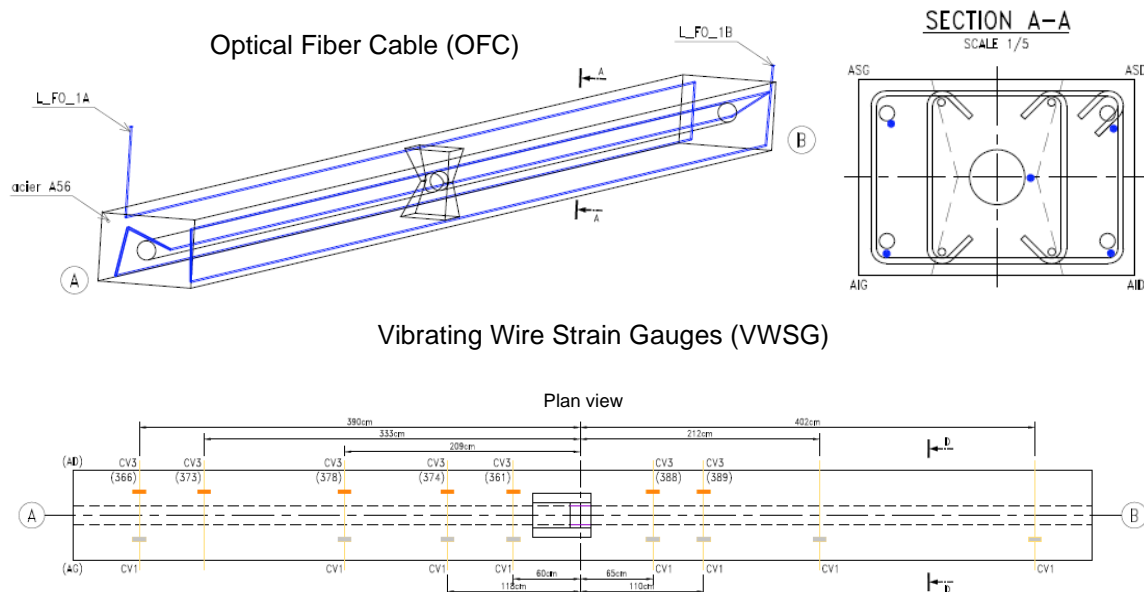
#### 4. Prestressed concrete beam - qualification for instantaneous concrete strain measurements for tendon rupture application

##### 4.1. Description of the test and objectives

The objective of this prestressed beam test is to experimentally study the re-anchoring phenomenon of a prestressing cable injected with cement grout within a smooth tube. This study is the continuation of a 2017 EDF test exploring innovative solutions for detecting the rupture of a prestressing cable, and was conducted in collaboration with Freyssinet.

The main goal is to quantify the ability of different strain measurement technologies to capture an instantaneous strain jump of decreasing amplitude (with a maximum close to the cutting area and converging towards 0 near the re-anchoring location) for different sensor technologies:

- Local strain measurement using Geo Instrumentation's SG1 (of the French Nuclear Power Plants) and Roctest EM3 (VWSG used on EPR Hinkley Point C), 15 sensors
- Distributed strain measurement by Optical Fiber Cable (AFL DNS4804 and Neubrex FN-EBSM cables), around 80m cumulative length



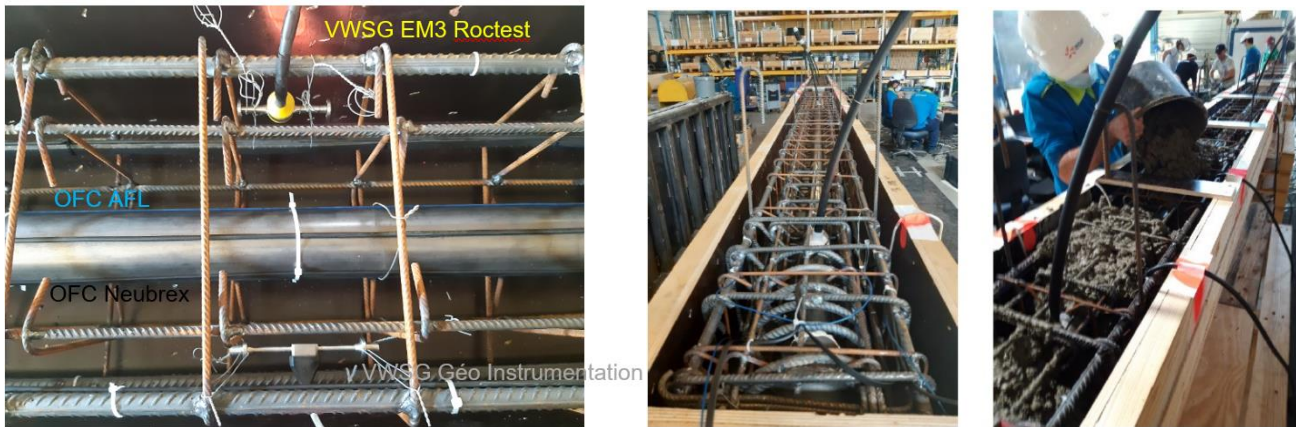


Figure 15: Drawings of the sensor arrangement and images of OFC and VWSG installed in the beam.

Highly resolved strain measurements (centimetric measuring step) are performed using a Rayleigh acquisition system (OBR 4600 Luna Technologies).

#### 4.2. Main results of the test

Figure 16 depicts the strain measurements along the beam after cutting the tendon, as recorded by the various sensors. From an instrumentation perspective, the following observations can be made:

- The various measuring systems used in this test (vibrating-wire extensometers, AFL and Neubrex Optical Fiber cables) were able to detect an instantaneous strain variation on the order of  $\pm 10 \mu\text{m/m}$  induced by the strand cutting,
- Excellent consistency is achieved in the measured strain values among the different systems along the entire length of the beam.
- The measurements exhibit excellent repeatability (this was assessed with 3 acquisitions for each strain variation) and residual deviation, confirming the high level of confidence in the obtained values,
- The calibrated values of the "extensometric coefficients" of the various strain measuring devices demonstrate a high level of metrological accuracy, as the differences observed between the different measurements systems are minimal,

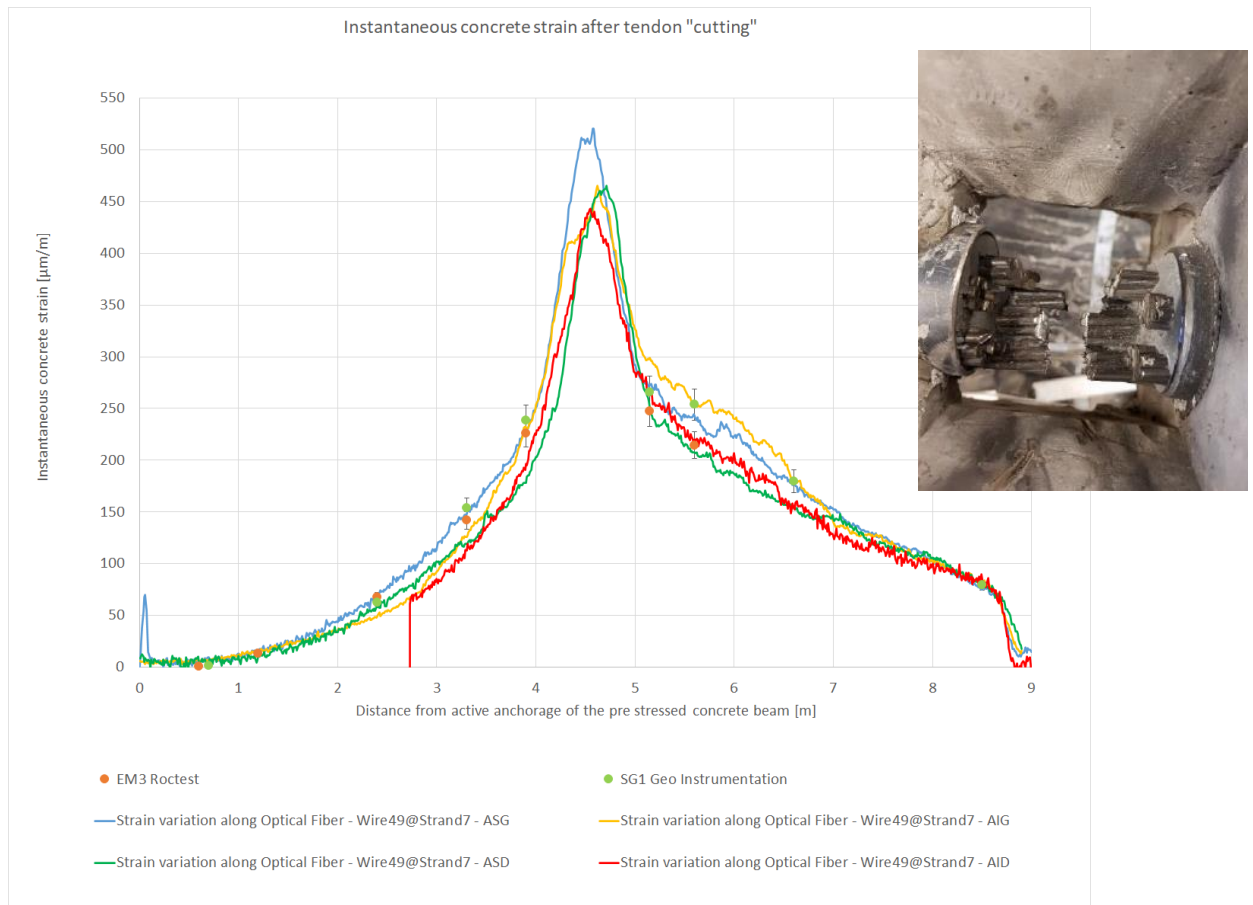


Figure 16: Concrete strain profile along the beam length after tendon cutting – comparison of OFC and VWSG measurements. The enclosed image shows the aspect of the cut tendon.

From a mechanical perspective, the measured re-anchorage appears asymmetric. On one side of the beam, it aligns with the re-anchorage length measured in a similar test in 2017 (with the only variable parameter being a ribbed sheath, while in this test a smoothed tube was used) and with the analytical calculation performed with Eurocode 2 formulae under the assumption of good bonding properties between the strand and the concrete (considering adapted equation 8.3 of Eurocode 2,  $l_{brqd,p} = \frac{\phi_p}{4} \frac{f_{y,p}}{\xi_1 f_{bd,p}}$ ) (Eurocode 2, 2005). On the other side of the beam, although the re-anchorage of the strand is clearly apparent, the measured re-anchorage length is notably longer, explaining the non-zero value at the right side ( $x=9m$ ) of Figure 17.

In the study, it is assumed that the anchorage length of the strands in the concrete corresponds to the length through which 97% of the load applied to the strands is transferred to the concrete. The strain of the concrete along the beam ( $x$ -axis) can then be expressed as  $\varepsilon(x) = \varepsilon(x_0)e^{-k(x-x_0)}$ , where  $\varepsilon(x_0)$  represents the maximum strain at the right of the rupture at  $x=x_0$ , and  $k$  is a characteristic parameter depending on the anchorage length  $k = -\ln(3\%)/l_{brqd}$  (assuming that 97% of the load applied to the strands is transferred to the concrete).

The work of Yuan (2005) on bonded assemblies supports the validity of this formula when the length of the structure exceeds the anchorage length. It should be noted that these formulations assume that materials and interface properties are homogeneous along the structure.

Adjusting the strain curves using the least squares method in accordance with the proposed model (Figure 20) enables experimental estimation of this anchorage length, measured at 3.2m on one side

(consistent with good bonding conditions according to Equation 8.3 of Eurocode 2 with  $\gamma_c = 1$ ,  $\eta_1=1$  &  $\xi=0.5$ ), and from 3.2m to 7.5m on the other side (corresponding to  $\eta_1 = 0.7$ ,  $\gamma_c=1$  &  $\xi\sim 0.2$ , closer to smooth rebar conditions).

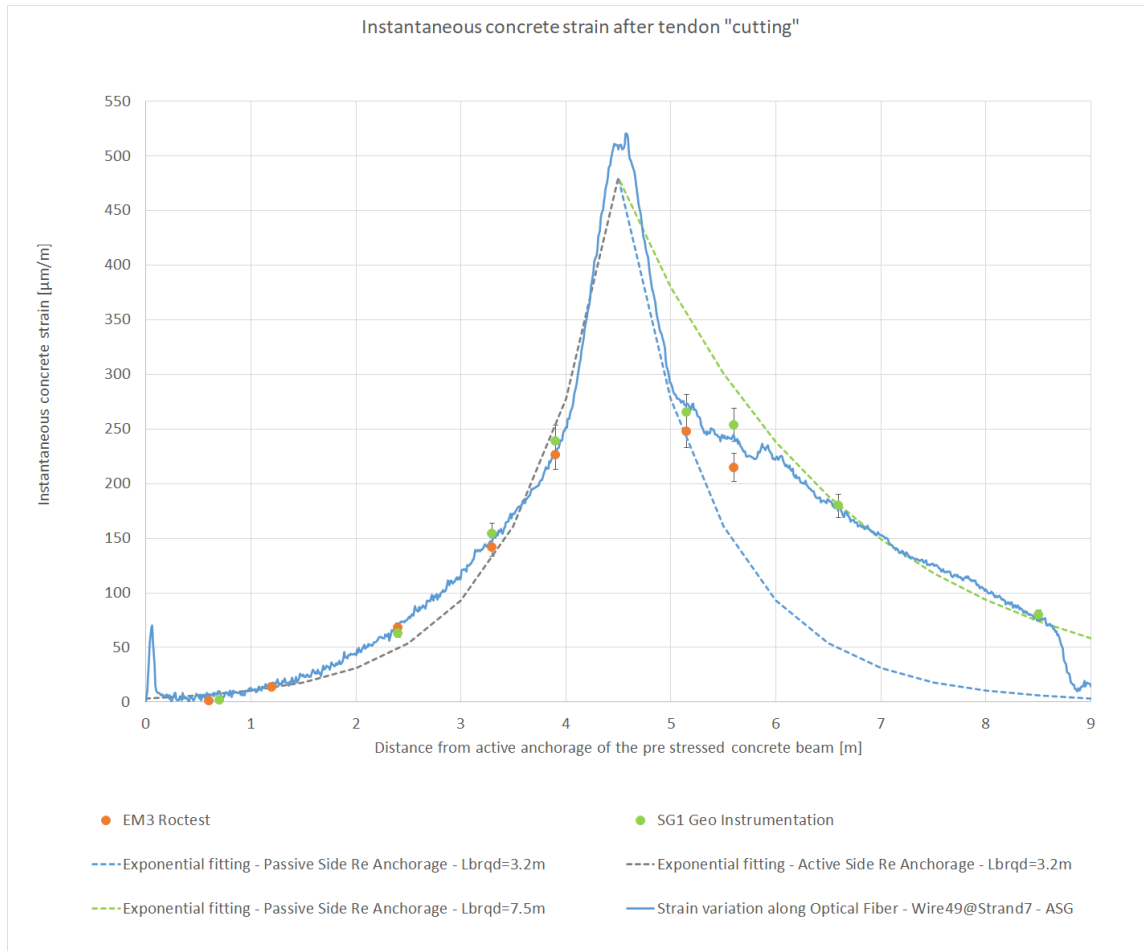


Figure 17: Concrete strain profile along the beam length after tendon cutting – Optical Fibers and VWSG measurements – exponential fitting for strand re-anchorage length measurement

Beyond the experimentally estimated anchorage length, the residual compression profile within the beam can be analyzed. The Optical Fiber system enabled experimental measurement of the re-anchoring of the strand after cutting, for a cement grouted strand in a smooth tube.

#### 4.3. Comparison between AFL and Neubrex OFC

The graphs in Figure 18 display the instantaneous concrete strain profile along the beam length measured just after tendon tensioning and after tendon cutting, as provided by AFL and Neubrex OFC. In both cases, good consistency is observed between the two cables.

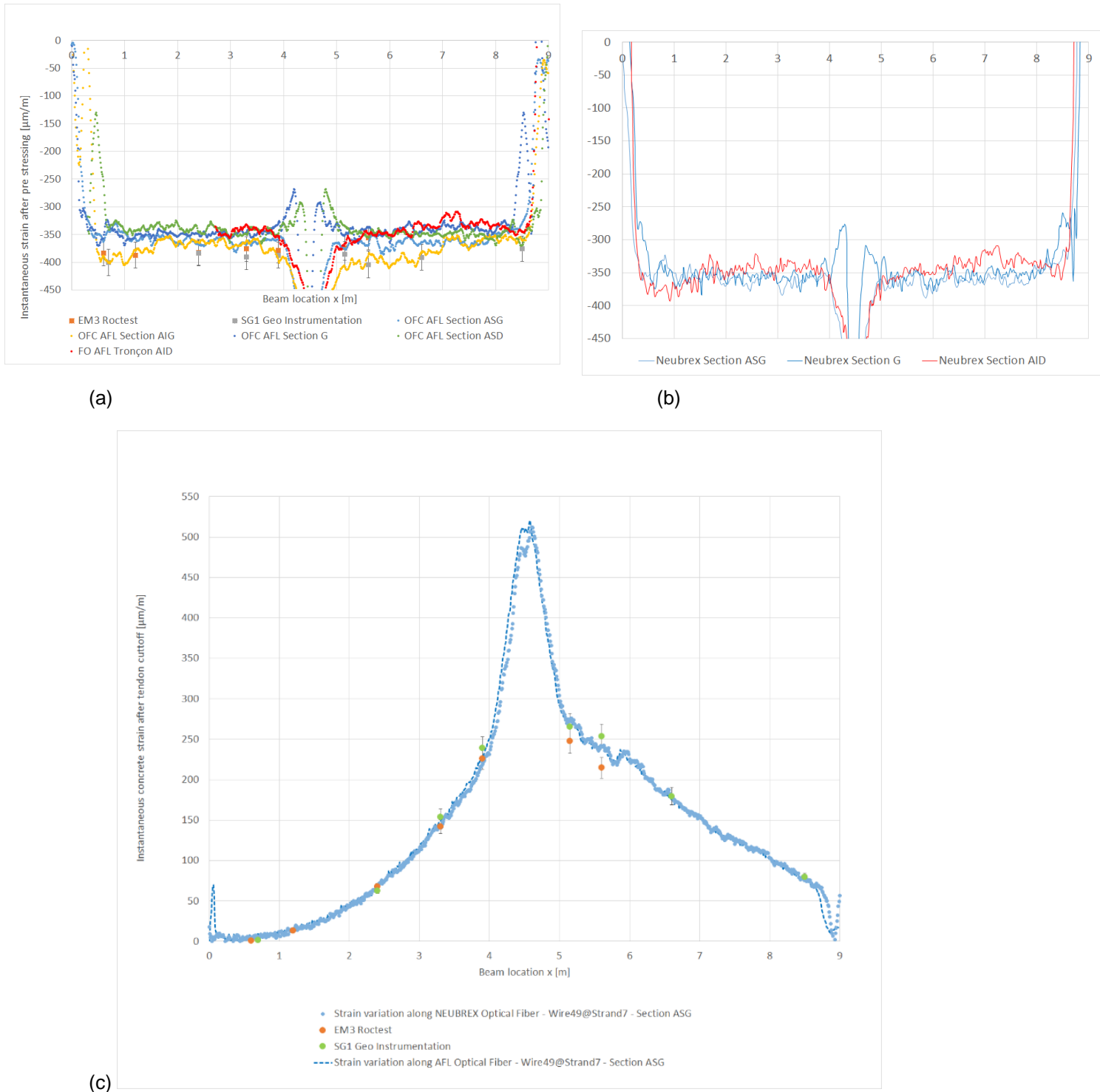


Figure 18: Instantaneous concrete strain profile along the beam length measured after tendon tensioning with AFL (a) Neubrex (b) cables, and after tendon cutting with both OFC (c).

## 5. Conclusion

On the VeRCoRs building, distributed monitoring systems enable quantitative analysis of the delayed and instantaneous concrete strains, respectively during operation and during the pressure tests. The conclusion is validated thanks to a comparison between distributed (Optical Fiber) and local (VWSG) extensometer technologies used for prestressing monitoring.



Thanks to the advantages of distributed strain monitoring provided by Optical Fiber technology it is possible to precisely analyze the mechanical behavior of the civil structure, in current area but also in specific regions near openings, where prestressing efficiency may be reduced, and stresses may be maximized.

On the tested prestressed beam with tendon cutting, the optical fiber systems can measure the re-anchorage of the tendon after cutting with a high level of confidence.

Reliable measurements appear to be achievable when the cable are embedded in concrete and also when it is externally bonded. For externally bonded OFC, measurement reliability appears to be more dependent on the specific cable used. Furthermore, we successfully identified glued configurations for all tested cables that produced results consistent with EDF metrological requirements for prestressed containment monitoring.

Durability aspects related to exterior conditions are currently under study, based on exposure tests conducted on OFC and adhesives.

The monitoring of distributed strains using Optical Fiber technology provides significant added value in the analysis of civil structure behavior. Potential applications in Civil Monitoring of Nuclear buildings can be considered include:

- New Build Projects (using embedded or externally bonded OFC)
- Existing structures (with surface-bonded OFC)

## **Acknowledgment**

The authors would like to recognize the contribution of Solenne Desforges and Jean Baptiste Claudet from EDF DTG in the tests performed on EDF concrete mockups.

Additionally, they are grateful to SITES company for their collaboration on VeRCoRs and to Freyssinet company for their collaboration on the prestressed beam test.

## **Disclosure Statement**

The authors report there are no competing interests to declare.

## **Data availability**

Due to the nature of the research, due to commercial supporting, data is not available.

## References

- Alj, I., Quiertant, M., Khaddour, A., Grando, Q. & Benzarti, K. (2022). Environmental Durability of an Optical Fiber Cable Intended for Distributed Strain Measurements in Concrete Structures. *Sensors*, 22(1), 141. <https://doi.org/10.3390/s22010141>
- Charpin, L., et al. (2022), Predicting leakage of the VERCORS mock-up and concrete containment buildings - a digital twin approach, *Acta Polytechnica CTU*, 33:78-84, <https://doi.org/10.14311/APP.2022.33.0078>
- Eurocode 2 (2005), Calcul des structures en béton NF EN 1992-1-1
- Galan, M., Simon, A., Guijarro, F., Reviron, N., Courtois, A. & Masson, B. (2022). Long-term measurement of concrete strains in pre-stressed containments: measurement uncertainty of the embedded vibrating wire strain gauges (vwsg) based on a 15-year laboratory testing campaign, *SMiRT-26 Berlin/Potsdam, Germany*, July 10-15, 2022. <https://www.lib.ncsu.edu/resolver/1840.20/40592>.
- Güemes, A., Fernández-López, A., Soller, B. (2010). Optical Fiber Distributed Sensing – Physical Principles and Applications, *Structural Health Monitoring*, 9, 233–245. <https://doi.org/10.1177/1475921710365263>.
- Henault, J.-M., Quiertant, M., Delepine-Lesoille, S., Salin, J., Moreau, G., Taillade, F & Benzarti K. (2012). Quantitative strain measurement and crack detection in RC structures using a truly distributed fiber optic sensing system. *Construction and Building Materials*, 37, pp. 916 – 923. DOI: 10.1016/j.conbuildmat.2012.05.029
- Henault, J.M., Salin, J., Moreau, G., Delepine-Lesoille, S., Bertand, J., Taillade, F., Quiertant, M. & Benzarti, K. (2011). Qualification of a truly distributed fiber optic technique for strain and temperature measurements in concrete structures. *EPJ Web of Conferences*, 12, 03004. DOI: 10.1051/epjconf/20111203004
- Naus, D. J. (2007), Primer on Durability of Nuclear Power Plant Reinforced Concrete Structures - A Review of Pertinent Factors, Oak Ridge National Laboratory, U.S. Nuclear Regulatory Commission, Office of Nuclear Regulatory Research, <https://doi.org/10.2172/931451>
- Oukhemanou, E., Desforges, S., Buchoud, E., Michel-Ponnelle, S & Courtois, A. (2016). VeRCoRs Mock-Up: Comprehensive Monitoring System for Reduced Scale Containment Model. *TINCE-2016*, Paris (France).
- Simon, A., Courtois, A., (2011), Structural monitoring of prestressed concrete containments of nuclear power plants for ageing management, *SMiRT-21 New Dehli, India*.
- Willm, G. & Beaujoint, N. (1967). Les méthodes de surveillance des barrages au service de la production hydraulique d'Electricité de France, problèmes anciens et solutions nouvelles, *IXth International Congress on Large Dams*, 1967, pp. 529–550
- Yuan, H. (2005). Improved theoretical solutions of FRP to concrete interfaces, *Proceedings of the international symposium on bond behaviour of FRP in structures* (BBFS 2005).